Available online at www.sciencedirect.com

ScienceDirect

Energy Procedia 89 (2016) 389 – 394

Energy Procedia

CoE on Sustainable Energy System (Thai-Japan), Faculty of Engineering, Rajamangala University of Technology Thanyaburi (RMUTT), Thailand

Simulation Study on Computer Tomography Imaging of Nuclear Distribution by Quasi Monoenergetic Gamma Rays with Nuclear Resonance Fluorescence: case study for ELI-NP application

I. Daito[a]*, H. Ohgaki[a], G. Suliman[b], V. Iancu[b], C. A. Ur[b], M. Iovea[c]

[a] *Institute of Advanced Energy, Kyoto University Goka-sho, Uji, kyoto 6110011, JAPAN*
[b] *Extreme Light Infrastructure – Nuclear Physics (ELI-NP)/Horia Hulubei National Institute for R&D in Physics and Nuclear Engineering (IFIN-HH), 30 Reactorului Street, P.O.B. MG-6, Bucharest-Magurele, Judet Ilfov, RO-077125, Romania*
[c] *Accent Pro2000, s.r.l., Nerva Traian 1, K6, Apt 26, Bucharest, S3, RO-031041, Romania*

Abstract

Non-destructive inspection carried out by using nuclear resonances excited by an MeV energy region gamma ray is a promising method. The high penetrability of MeV gamma ray of nuclear resonant energy makes possible the detection of nuclides surrounded by massive materials. As an application of this method, computed tomography imaging of nuclear distribution inside objects can be reconstructed from transmission factor of gamma rays. We have studied the image reconstruction of the nuclear distribution using Monte-Carlo simulations to estimate the gamma-ray transmission factor assuming the ELI-NP facility where about 3 order higher intensity of quasi-monoenergetic gamma rays will be available.

Peer-review under responsibility of the organizing committee of the 12th EMSES 2015

Keywords: Laser Compton Scattering; Nuclear Resonance Fluorescence; non-destructive inspection; Computed Tomography

1. Introduction

An MeV energy region gamma-ray is a good probe for non-destructive inspection of high density and massive objects because of its high penetrability. Because of the weak element dependence of attenuation coefficient in this energy regime, it is possible to know the mass distribution. Moreover, it is possible to detect the presence of a

* Corresponding author. Tel.: +81-774-71-3485; fax: +81-774-71-3316.
E-mail address: daito.izuru@gmail.com

Peer-review under responsibility of the organizing committee of the 12th EMSES 2015
doi:10.1016/j.egypro.2016.05.051

specific nuclide by the process of nuclear excitation, provided that the energy of the incident gamma ray is equal to the excitation energy of the nuclear resonance state (Nuclear Resonance Fluorescence: NRF) of the target nucleus. A non-destructive inspection of Special Nuclear Materials (SNMs) hidden in a container cargo using NRF is proposed by Bertozzi [1] for the nuclear non-proliferation and prevention of the nuclear terrorism. Several developments have been carried out at many institutes for SNM detection systems [2-4] and non-destructive detection of Plutonium and other nuclear products inside of a spent nuclear fuel rod [5,6]. For NRF experiments, a Laser Compton Scattering (LCS) gamma-ray beam, which can generate energy tunable and quasi-mono energetic gamma rays, is an ideal gamma-ray source. Quasi-mono energetic gamma-rays suppress a number of off-resonant energy gamma-rays which make the huge background events at the foot of NRF gamma-rays caused by atomic processes i.e. Compton- and Rayleigh-scattering and so on.

Images of the density and nuclear distributions inside objects can be reconstructed from one-dimensional distribution of the off-resonance transmission factor by Computed Tomography (CT) [7] and on-resonance (NRF) scattering technique [8]. However, the intensity of existing LCS gamma-ray beams [9-11] is not high enough to obtain a nuclear distribution image reconstruction from the NRF method. Currently, a new LCS gamma-ray facility is being built as part of the Extreme Light Infrastructure-Nuclear Physics (ELI-NP) [12] in Romania and will deliver one of the brightest and highest quality LCS gamma-ray source. The designed flux of the collimated gamma-ray beam is in the range of 10^8 ph/s with the energy spread of 0.5 % in standard deviation. The non-destructive imaging of density and nuclear distribution is part of a proposal for industrial application research at ELI-NP [13].

In this work, we made a feasibility study of reconstruction of a CT image of density and nuclear distribution of ^{238}U surrounded by high density materials in ELI-NP. The gamma-ray beam parameter and the detection system are taken from Ref. [13]. A modified version of GEANT4, which takes into account all NRF processes, developed by our group [14] was employed for this work, because the NRF process was not included in an original GEANT4 code [15].

2. Nuclear Resonance Fluorescence

NRF is a process in which a nucleus absorbs energy from gamma rays and is excited to a nuclear state of higher energy. Subsequently, the excited nucleus emits one or more gamma rays to de-excite to the ground state (Fig. 1). The excitation energy of the resonant state is specific to each nuclide. By irradiating nuclei with gamma rays of energy Existence of the NRF gamma rays or decrease of gamma-ray intensity at the resonant energy which pass through a measured object show the presence of the nuclide in the object. The natural width of the NRF resonances is usually equal to the nuclear excitation energy, a resonant absorption of the gamma ray occurs only in the nuclide of interest. Existence of the NRF gamma rays or decrease of gamma-ray intensity at the resonant energy which pass through a measured object show the presence of the nuclide in the object. The natural width of the NRF resonances is usually quite narrow, being less than 100 meV. However, because of thermal motion of the nucleus, the width of the resonance is typically of the order of eV. Therefore a mono energetic gamma-ray beam with high spectral density is desired for realistic applications of the NRF. In this work, we performed Monte Carlo simulations to

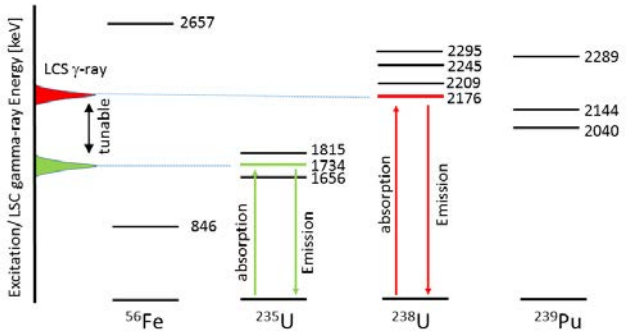

Fig. 1. A schematic drawing of the NRF process excited by LCS gamma-ray beam.

detect ^{238}U nuclide in a thick, massive object. The resonance width employed was 1.78 eV for 2176 keV state of ^{238}U at 300 K. In these simulations, the employed energetic resonant shape of cross section $\sigma(E_\gamma)$ is described by an equation of

$$\sigma(E_\gamma) = \frac{\sigma_{total}}{\sigma\sqrt{\pi}} \exp\left(\frac{-(E_\gamma - E_0)}{\sigma^2} \right) \quad , \tag{1}$$

where, σ_{total} is the integrated absorption cross section, E_0 is the centroid energy of the resonance and δ is the width of the resonance. In this work: $\sigma_{total} = 82.7\ b \cdot eV$ and $\delta = 1.78\ eV$ [16]. The branching ratio of de-excitation is 65.8 % to the ground state and 34.2 % to first excited state (excitation energy of 44.9 keV).

3. Laser Compton Scattering

Laser Compton scattering gamma ray is generated by collision between relativistic electron and laser photon. By colliding, the electron kinematic energy is transferred to the recoil photon and the frequency of the photon is up-shifted. The energy of recoiled photon is given by the equation [17]:

$$E_\gamma(E_e, E_l, \varphi, \theta) = \frac{E_l(E_e - p_e \cos\varphi)}{E_l(1 - \cos(\theta - \varphi) + (E_e - p_e \cos\theta))} \tag{2},$$

where, E_γ is the generated gamma-ray energy, E_l is the laser photon energy, E_e is the electron energy, p_e is the electron momentum, φ and θ are the incident and the scattered angle of the photon, respectively. The energy of the gamma ray is defined only by its scattering angle when the incident angle of laser photon is fixed. Thus, a quasi-monoenergetic gamma-ray beam is obtained by defining its scattering angle by a narrow collimator.

4. Simulation Set up

In this study we adopted the NRF transmission method [16] to obtain the transmission factor of the LCS gamma rays and to reconstruct a CT image. A schematic drawing of the simulation set up is shown in Fig. 2(A).

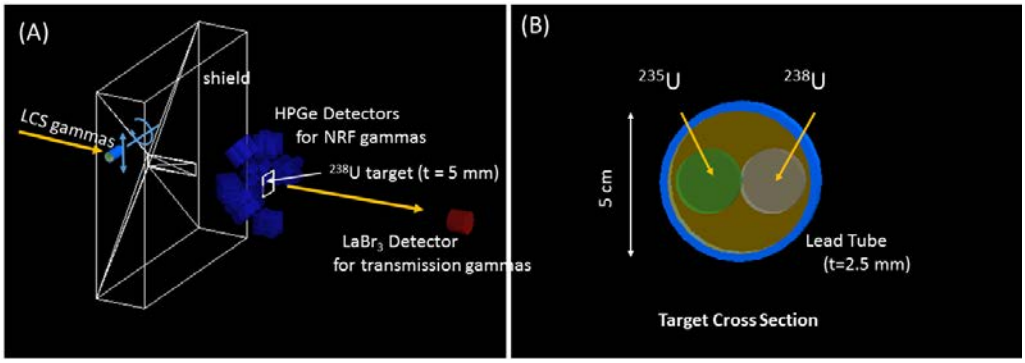

Fig.2. (A) A schematic drawing of target and detectors layout. LCS gamma-rays came from the left side of the figure. 32 HPGe detectors for NRF gamma-ray detection are protected by a 25 cm lead wall from radiations from the measured object. The transmission factor of the incident gamma rays at the resonant energy of ^{238}U is measured by NRF gamma rays scattered on the "Notch target" (^{238}U) located at a downstream of the lead shield wall. The attenuation of whole gamma-rays are also measured by a $LaBr_3$ detector installed downstream on the beam axis. (B) A cross section view of the measured object. The outer diameter of lead tube is 5 cm and its thickness is 2.5 mm. Inside the tube, 2 cm thick ^{235}U and ^{238}U rods are inserted and the tube is filled with gallium.

LCS gamma-ray beam impinge from the left side of the figure. The gamma rays irradiate the measured object located on the beam axis. The object was rotated around the horizontal axis and moved vertically to obtain projection images.

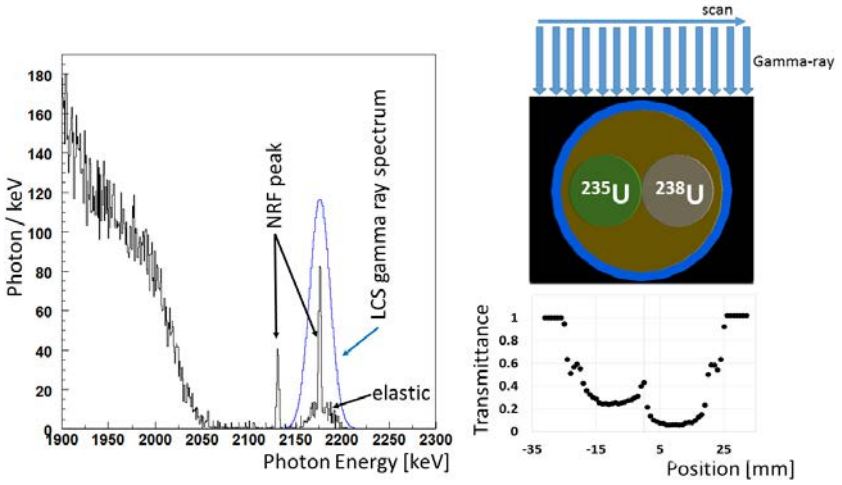

Fig.3. (left) Typical energy spectra around NRF resonance energy obtained by irradiating with quasi-monoenergetic gamma rays. The two narrow peaks are NRF peaks and the wide peak at the foot of higher NRF peak represents the elastic scattered gamma rays. The blue line in indicates the incident photon energy distribution. It is clearly possible to separate the NRF peak from the elastic scattering peak. (right) An example of on-resonance energy gamma-ray transmittance distribution (projection image) obtained by scanning the measured object. The gray circle indicates the ^{238}U rod. Because of the NRF process, the transmittance of ^{238}U rod is lower than that of ^{235}U rod. By rotating the object, 12 projection images are obtained.

Downstream of the object, a 25 cm thick lead wall was installed to shield the gamma-ray detectors from radiations scattered from the measured object. The wall had a through hole on the beam axis for gamma rays, which were transmitted through the object. A notch target was located behind the wall. The resonance width of the NRF state of ^{238}U is 1.78 eV, which is quite narrower than the energy resolution of gamma-ray detectors. Therefore, the decrease of gamma-ray intensity at the resonant energy was measured by NRF scattering on the notch target. The notch target consists of pure ^{238}U and its thickness is 5 mm. The attenuation of the gamma ray at the resonant energy was measured by counting the NRF gamma rays from ^{238}U in the notch target. According to the ELI-NP design, a segmented High Purity Germanium (HPGe) clover detectors roughly equivalent to 16 crystals at 90 degree and 16 HPGe crystals at 135 degree will be installed. The diameter of the Ge crystal is 6 cm and its length is 9 cm. A cross section of the measured object is shown in Fig. 2(B). The object consists of a 5 cm outer and a 4.5 cm inner diameter lead tube (density ρ = 11.34 g/cm^3, attenuation coefficient $-\mu/\rho = 4.606 \times 10^{-2}$ g/cm^2) and 2 cm thick ^{235}U and ^{238} U rods (ρ = 18.95 g/cm^3, $-\mu/\rho = 4.878 \times 10^{-2}$ g/cm^2). All the space between the tube and these rods was filled with gallium (ρ = 5.904 g/cm^3, $-\mu/\rho = 4.113^{-2}$ g/cm^2).

To simulate the density distribution measurement, we calculated the transmission of the whole incident gamma-ray beam (centroid energy of 2176 keV and energy spread of 0.5 % in standard deviation). The incident photon number used in the simulation was 10^6 for each measurement. The transmission factor was evaluated from the energy deposit of on- and off-resonance photons arrived at the $LaBr_3$ detector.

On the other hand, the fraction of gamma rays with energy within the resonance width is only ~10^{-4}. A typical gamma ray spectrum detected by HPGes is shown in left panel of Fig 3. In the spectrum, a continuum (up to 2050 keV), two narrow peaks of NRF gamma rays and an elastic scattering peak at the foot of higher NRF peak are observed. The peak at higher energy corresponds to the gamma rays emitted following the transition to the ground state and the lower one is to the 1st excited state. The width of the elastic scattering peak, which is equal to that of the incident beam is quite different than that of the NRF peak, therefore it is clearly possible to separate the NRF

peak from the elastic scattering peak. Thus, for the attenuation measurement at NRF resonant energy, 10^6 monoenergetic gamma rays were used to reduce the computation time. The incident photon number was equivalent to 100 sec of ELI-NP beam time. In the simulation, by scanning along the vertical direction. The transmittance was measured at every 15 degree by rotating the measured object and every 1 mm (64 points) following the transition to the ground state and the lower one is to the 1st excited state. The transmission factor at NRF resonant energy was obtained from the yields of the narrow peaks. An example of obtained projection image is shown in the right panel of Fig. 3.

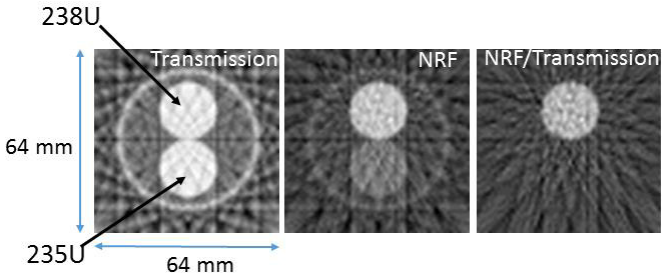

Fig.4. Cross section images obtained by whole beam transmission factor (left panel) and by NRF gamma rays (middle). Right panel image is reconstructed using the ratio of NRF gamma strength to transmittance of whole energy gamma ray. In the figures, white parts are equivalent to parts of strong gamma-ray attenuation.

5. CT Image Reconstruction

CT image reconstruction was obtained using the filtered back projection method from twelve (one dimensional) projection images. The filter employed was the Shepp-Logan filter. The reconstructed images are shown in Fig. 4. In the figures, the large attenuation part is expressed with white color. The left panel of Fig. 4 shows a density distribution obtained by whole gamma-ray transmission factor, a standard CT image of the density distribution. The middle panel is reconstructed by the transmission factors of on-resonance energy. ^{238}U rod is clearly enhanced compare with ^{235}U rod. However, because of the gamma rays attenuation by other processes than NRF, other materials are also visible. These attenuations can be removed by evaluating the whole energy spectrum, which is equivalent to the total transmission of the measured object. Because of the weak energy and element dependence of attenuation coefficient, the coefficient and density along the beam axis can be described by average value $(\mu/\rho)_{ave}$ and ρ_{ave}. Thus, a transmission factor of on-resonance gamma ray is written by an equation of

$$\varepsilon_{ON} = \exp\left[-\left(\left(\mu/\rho\right)_{ave}\cdot\rho_{ave} + \sigma_{NRF}\cdot\rho_{NRF}\cdot N_A / M_{NRF}\right)L\right] , \quad (3)$$

where L is the distance from source to the notch target, M_{NRF} is the atomic mass of nuclide to measure, and N_A is the Avogadro number. For the off-resonance gamma ray, σ_{NRF} is zero, then transmission factor of the off-resonant energy is

$$\varepsilon_{OFF} = \exp\left(-\left(\mu/\rho\right)_{ave}\cdot\rho_{ave}\cdot L\right) . \quad (4)$$

Therefore, from eq. (3) and eq. (4), the ratio of $\varepsilon_{ON}/\varepsilon_{OFF}$ only depends on ρ_{NRF} which is the deduced NRF absorption of the measured object (right pannel of fig 4). Consequently, we can clearly obtain the image of the ^{238}U rod and we propose this enhancing method to visualize the isotope distribution. In terms of feasibility of taking a CT image of a nuclear distribution of ^{238}U surrounded by high density materials at ELI-NP, the required data acquisition time is estimated to be 21 hours for 12 scanning angles and 64 views.

The required quality of the nuclear distribution image is totally dependent on the actual application. However, we conclude that the proposed method to obtain a CT image of a nuclear distribution inside an object could be feasible at ELI-NP.

6. CONCLUSION

A simulation study of the CT imaging of nuclear distribution by NRF processes induced by quasi-monoenergetic LCS gamma rays was performed by employing a Monte-Carlo simulation code GEANT4. The specifications of the gamma-ray beam is based on the design value of LCS gamma-ray beam at ELI-NP. The nuclear distribution image is reconstructed by measuring the transmittance of on- and off-resonance energy of gamma rays through an object. ^{238}U hidden in dense materials is clearly visualized using the transmission factor of on-resonance gamma rays normalized by that of off-resonance gamma ray.

ACKNOWLEDGMENT

This work was supported by JSPS KAKENHI Grant Number 26289363 and Memorandum for Scientific Collaboration on the Implementation of the Extreme Light Infrastructure-Nuclear Physics (ELI-NP) Project between Horia Hulubei National Institute for R&D in Physics and Nuclear Engineering (IFIN-HH), Romania and the Institute of Advanced Energy, Kyoto University, Japan. The ELI–NP project is co–funded by the European Union through the European Regional Development Fund.

References

[1] W. Bertozzi and R. J. Ledoux, Nucl. Instru. Meth. B, vol. 241, pp. 820-825 (2005).
[2] J. Pruet *et al*., J. Appl. Phys. 99, 123102 (2006)
[3] C. A. Hagmann *et al.*, J. of Appl. Phys.106, 084901 (2009).
[4] H. Ohgaki *et al*., Proc. of IEEE HST 2012, pp.666-671, 2012.
[5] R. Hajima *et al*., Journal of Nuclear Science and Technology 45 (5), 441-451 (2008).
[6] B. Ludewigt, V. Mozin, A. Haefner, B. Quiter, Proceedings of the 2010 ANS annual meeting, San Diego, California (2010).
[7] H. Toyokawa *et al*., Proc. Part. Acc. Conf. 713 (2003).
[8] H. Toyokawa *et a*l., Japanese Journal of Applied Physics 50, 100209 (2011).
[9] H. Ohgaki *et al*., Nucl. Inst. Meth. Phys. Res. A, vol. 455, pp. 54-59 (2000).
[10] S. Miyamoto *et al.*, Radiation Measurements, vol. 41, S179–S185 (2007).
[11] H.R. Weller *et al.*, Prog. Part. Nucl. Phys., vol. 62, 257-303 (2009).
[12] The White Book of ELI Nuclear Physics, Bucharest-Magurele, Romania (2011).
[13] Gamma Beam Industrial Applications at ELI-NP, Technical Design Report, in press.
[14] H. Negm et al., Journal of Nuclear Science and Technology, (2014) http://dx.doi.org/10.1080/00223131.2014.980348
[15] S. Agostinalli *et al*., Geant4-a simulation toolkit, Nucl. Instr. Meth. Phys. Res. A, 506, 250(2003)
[16] B. A. Ludewigt, B. J. Quiter, and S.D. Ambers, Nuclear Resonance Fluorescence for Safeguards Applications, DOE report, http://dx.doi.org/10.2172/1022713 (2011).
[17] F. R. Arutynian and V. A. Tumanian, Phys. Lett. vol.4 pp.176-178 (1963).